

Probing the evolution of slow flow dynamics in metallic glasses

P. Luo, Z. Lu, Y. Z. Li, H. Y. Bai, P. Wen,^{*} and W. H. Wang[†]

Institute of Physics, Chinese Academy of Sciences, Beijing 100190, People's Republic of China

(Received 13 August 2015; published 21 March 2016)

The dynamics of glass is of paramount importance for understanding glass, while experimental studies of it covering broad time and temperature ranges are fraught with difficulty. We employ a method which can probe the extremely slow dynamics in various glassy states in metallic glass (MG). The flow dynamics of as-cast MG is found to follow a universal Arrhenius behavior in a wide temperature range, and aged MG follows a stretched exponential function with a “magic” exponent number of $3/7$. Our observations have implications for understanding the structural evolution of the slow flow and the issue of finite temperature divergence in MGs.

DOI: [10.1103/PhysRevB.93.104204](https://doi.org/10.1103/PhysRevB.93.104204)

Upon cooling a liquid, the structural relaxation time gradually increases and the corresponding flow becomes more and more difficult, and eventually the liquid loses its ability to flow on the laboratory time scale and a nearly rigid glass is thus obtained. A popular myth concerning the apparent flow of medieval stained glass windows has attracted substantial attention and discussion on whether glass flows at low temperature [1]. On the other hand, a general problem of whether the finite temperature divergence of relaxation time exists is actively debated in the glass science community [2]. Relaxation behavior has been the center of understanding the nature of glass and supercooled liquid (SL), and presents one of the most challenging unsolved problems in condensed matter physics [3–6]. Recently, the intrinsic correlation between microscopic glass relaxation and macroscopic detectable flow on long experimental time scales has been revisited [7], resulting in an opportunity to understand the nature of glass and SL in depth.

Metallic glasses (MGs), with a structure viewed approximately as a dense random packing of hard spheres [8], offer a simple but effective model system for the study of some controversial issues in glasses. Relaxations in MGs have been found to be closely bound to mechanical behaviors [9–14] as well as to localized atomic diffusion [15]. Nevertheless, in-depth understanding of the intrinsic relaxation mechanism and the extremely slow flow phenomenon in MGs remain elusive due to the lack of coverage of broad time and temperature ranges in previous studies [16–21]. Recently, we developed a mandrel winding method which can realize homogeneous flow in MGs [9]. By mandrel winding, the strain of MG ribbons can be manifested in the form of the diameter D of a helical shape, and thus minor strain change induced by the winding can be visually shown and precisely measured. With this method the heterogeneous deformation (e.g., localized shear bands) [22,23] can be avoided, and the homogeneous plastic flow in MG is thus achieved. Moreover, long time and wide temperature observation for flow is available, enabling us to study the slow homogeneous flow and the corresponding intrinsic dynamic mechanism in MGs far below the glass transition temperature T_g .

In this work, we scrutinize the evolution of the flow behaviors of MGs from T_g to room temperature (RT) via the mandrel winding method. We show that the flow behaviors in as-cast and aged MGs are totally different. The flow dynamics of as-cast MG follows a universal Arrhenius behavior in the whole wide temperature range investigated. Aging treatments have significant effects on the evolution of flow behaviors. For properly aged MGs, the flow behavior follows a stretched exponential form with a “magic” number ($3/7$). The evolution of the flow behaviors as well as the atomic configurations’ change of flow units during aging is discussed.

Four typical MGs of $Zr_{50}Cu_{40}Al_{10}$ ($T_g = 693$ K), $Y_{60}Ni_{20}Al_{20}$ ($T_g = 588$ K), $La_{55}Ni_{20}Al_{25}$ ($T_g = 473$ K), and $Gd_{55}Al_{25}Cu_{10}Co_{10}$ ($T_g = 578$ K) were utilized. Glassy ribbons with a uniform thickness of ~ 22 μm were prepared by a melt spinning method (see the Supplemental Material [24] for details). As illustrated in Fig. 1(a), the ribbons were helically wound around a stainless steel mandrel with a diameter of 3 mm. The fully wound states were mechanically constrained (Fig. S1 [24]) and placed in a furnace for a period of holding time t at a certain temperature T , and then released from the mandrel. Temperature fluctuations during the experiments did not exceed 0.5 K. The outer diameter D of the released ribbon was measured to determine the residual strain that exhibits the effective flow actually taking place. Controlling the holding time t , soak temperature, and heat treatment condition, one can trace a complete evolution of the slow flow behavior in given samples without crystallization (Fig. S2 [24]). For a wound ribbon, the maximum strain on the surface is estimated as $\varepsilon = \frac{d}{D-d}$, where d is the ribbon thickness. The initial imposed maximum strain ε_i was calculated to be 0.728% (within the elastic regime). After applying a constraint for t at T , the maximum strain $\varepsilon_T(t)$ of the released ribbon is obtained. For comparison, a scaled strain of $\varphi_T(t) = \frac{\varepsilon_T(t)}{\varepsilon_i}$ was employed as a parameter to characterize the flow process. We designate $\varphi_T(t)$ as the degree of flow; that is, partial flow is expressed as $\varphi_T(t)$, which is less than unity, and complete flow is achieved if $\varphi_T(t) = 1$. As shown in Fig. 1(b), $\varphi_T(t)$ is measurable in the released ribbons after being helically wound and held in place around a mandrel at $0.6T_g$ for different times. No shear band can be found on the released ribbons [Fig. 1(c)], confirming that such pronounced flow is homogeneous.

Figure 2(a) illustrates the temporal evolution of flow processes occurring in as-cast MG samples at various temperatures (scaled by T_g for comparison). The degree of flow varying

^{*}pwen@iphy.ac.cn

[†]whw@iphy.ac.cn

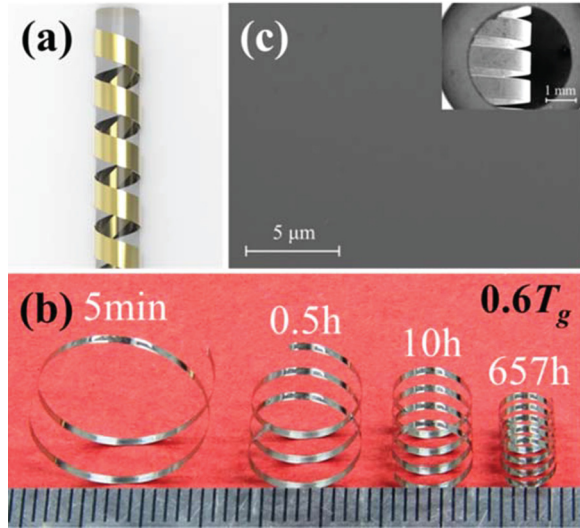


FIG. 1. (a) The helical mandrel winding method. (b) The released $Zr_{50}Cu_{40}Al_{10}$ MG ribbons after being helically wound and held in place at $0.6T_g$ for different times. (c) A scanning electron microscopy image of the surface topography of a released $Zr_{50}Cu_{40}Al_{10}$ MG ribbon after being wound and held in place at $0.6T_g$ for 657 h.

in the measuring time window has a common feature. The variation of $\varphi_T(t)$ with t can be divided into two distinct stages: a rapid increase within the incipient short-time region and the following universal long-time region where $\varphi_T(t)$ slows down but persistently advances in a linear form with logarithmic time. Moreover, at the same scaled temperature for all investigated MGs, the $\varphi_T(t)$ in the long-time region follows nearly the same trace within the experimental sensitivity. Likewise, for different mandrel D values (e.g., $Zr_{50}Cu_{40}Al_{10}$ MG with $D = 3$ and 6 mm), $\varphi_T(t)$ can collapse onto one curve, independent of the initial imposed strain or stress. Thus, it is reasonable to deem that the slow flow in MGs depends on the intrinsic relaxation of glass, regardless of external driving stress. Namely, the method utilized is just a perturbation for glass, similar to the usually used dynamic mechanical methods, where a perturbation is given to the material and its relaxation behavior in the frequency domain is detected. As the wound material is held in place at T , with time going on, the atoms rearrange their positions driven by the stored elastic energy, resulting in a residual strain after release. If the holding time t is long enough, each individual atom can find its most comfortable place where the elastic energy is depleted, and the released ribbon no longer shows any recovery, and the flow process from a straight ribbon to a helical shape is completed [$\varphi_T(t) = 1$]. The change of D reflects, microscopically, the rearrangement of atoms within the glass, and is an indicator for the relaxation time.

From $0.5T_g$ to $0.8T_g$, the flow advances linearly with logarithmic time, and we can thus derive a characteristic time t_c from the available data to mark the complete flow. The temperature dependence of t_c is found to follow the Arrhenius behavior, $t_c = t_c^\infty \exp[\frac{\Delta E_a}{k_B T}]$, with a prefactor $t_c^\infty = 10^{-13.03 \pm 0.73}$ s and an activation energy of 1.93 ± 0.07 eV [Fig. 2(b)]. On the other hand, through time-temperature superposition [25], the Arrhenius law is also satisfied and the activation energy is determined to be 1.90 ± 0.04 eV

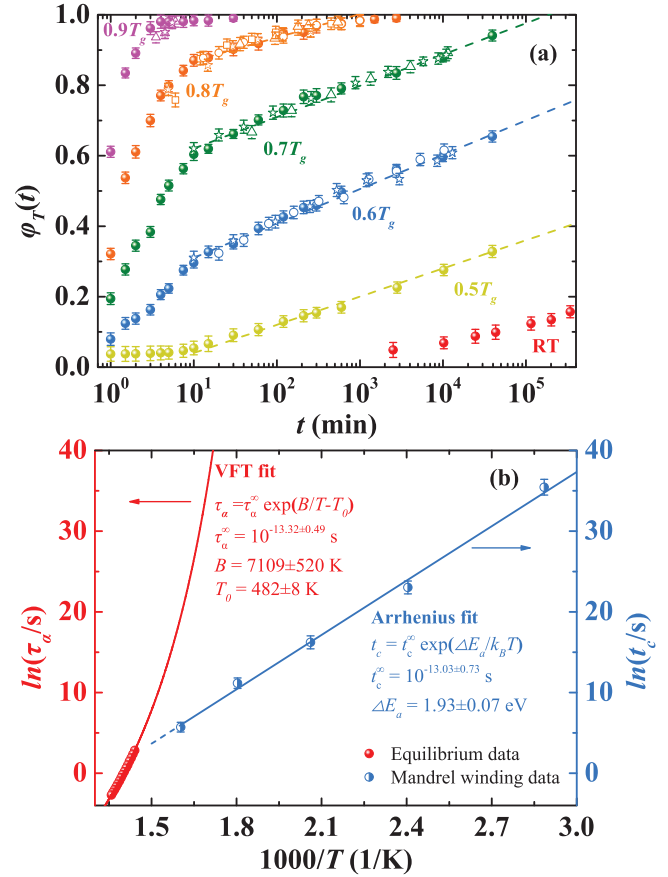


FIG. 2. (a) Temporal evolution of scaled strain of four MG systems at different temperatures (scaled by T_g): $Y_{60}Ni_{20}Al_{20}$ (\star), $Gd_{55}Al_{25}Cu_{10}Co_{10}$ (Δ), $La_{55}Ni_{20}Al_{25}$ (\square), and $Zr_{50}Cu_{40}Al_{10}$ (\bullet) with a mandrel diameter of 3 mm; $Zr_{50}Cu_{40}Al_{10}$ MGs with a mandrel diameter of 6 mm are also shown (\circ). The scaled strain data were obtained from the average of three individual measurements under the same conditions. The dashed lines show a linear fit to the raw data with a holding time longer than 10 min. (b) Characteristic time t_c for complete flow and structural relaxation time τ_α of SL of $Zr_{50}Cu_{40}Al_{10}$ MGs against the inverse temperature. The light blue line is an Arrhenius fit, and the red line is a VFT fit.

(Fig. S3 [24]), reasonably equal to that calculated from the temperature-dependent t_c . Moreover, t_c and ΔE_a have a close relationship with the relaxation time τ_α and the activation energy of structural relaxation in SL. As shown in Fig. 2(b), the curve of t_c can be extended to match τ_α , measured by a dynamical mechanical analyzer (Fig. S4 [24]). A fit of the Vogel-Fulcher-Tammann (VFT) function [26], $\tau_\alpha = \tau_\alpha^\infty \exp[\frac{B}{T-T_0}]$, to the equilibrium relaxation time gives $\tau_\alpha^\infty = 10^{-13.32 \pm 0.49}$ s, $B = 7109 \pm 520$ K, and $T_0 = 482 \pm 8$ K. Keeping τ_α^∞ , we obtain the activation energy of the structural relaxation in SL by transforming the VFT function into an Arrhenius expression, and find that the activation energy for the complete flow in glass is in accordance with that of the structural relaxation of SL (Fig. S5 [24]), indicating that the flow in as-cast MG has an intrinsic correlation with the relaxation of SL.

Glass is thermodynamically unstable, continually relaxing toward an equilibrium state (i.e., physical aging) [27]. Further exploration of the flow behavior in glasses with different

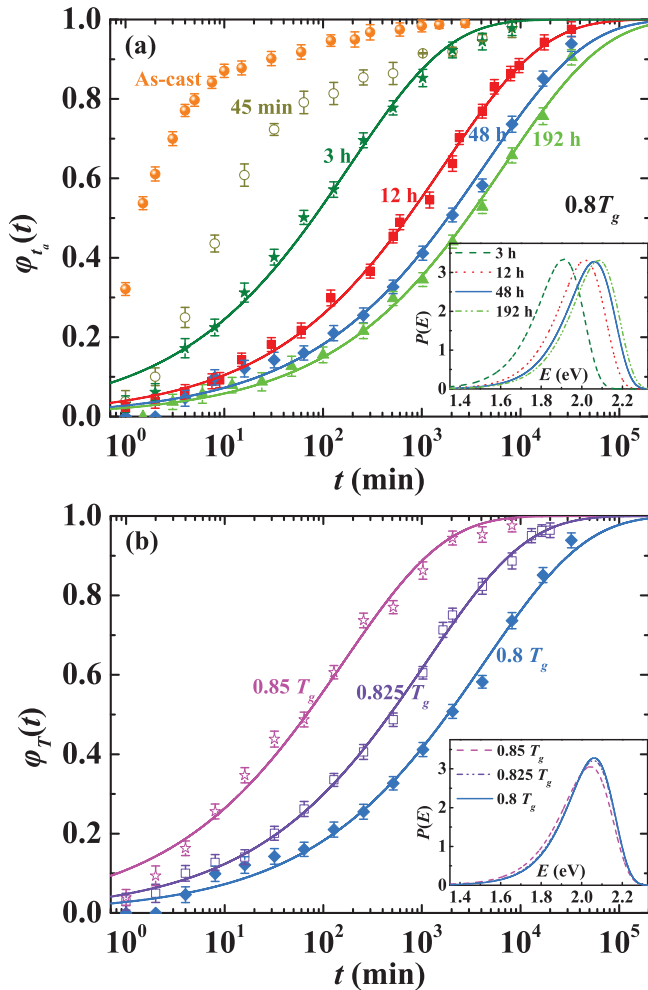


FIG. 3. (a) Temporal evolution of scaled strain of Zr₅₀Cu₄₀Al₁₀ MGs preaged at $0.8T_g$ for different times. The mandrel winding temperature is $0.8T_g$. The lines represent the fit of a stretched exponential function. The stretching exponents are 0.434 ± 0.022 , 0.431 ± 0.008 , 0.426 ± 0.015 , and 0.431 ± 0.013 for preaging of 3, 12, 48, and 192 h, respectively. (b) Temporal evolution of scaled strain of Zr₅₀Cu₄₀Al₁₀ MGs preaged at $0.8T_g$ for 48 h, at different mandrel winding temperatures. The lines represent the fit of a stretched exponential function. The stretching exponents are 0.426 ± 0.023 and 0.430 ± 0.008 for $0.85T_g$ and $0.825T_g$, respectively. All of the stretching exponents are nearly equal to $3/7$. The insets in (a) and (b) show corresponding activation energy spectra $P(E)$.

energy states induced by aging may deepen our understanding of the intrinsic mechanism of slow flow dynamics. We examined the flow behaviors of Zr₅₀Cu₄₀Al₁₀ MGs preaged at $0.8T_g$ for different times (t_a) before mandrel winding. As shown in Fig. 3(a), the flow behavior at $0.8T_g$ varies dramatically after preaging. Upon annealing, the characteristic time t_c increases and the flow changes gradually into a stretched exponential form $\phi_{t_a}(t) = 1 - \exp[-(t/\tau)^\beta]$. More intriguingly, the stretching exponents coincide, univocally, with a particular value of $3/7$, which is the characteristic value of β for relaxation dominated by long-range pathways in the diffusion-trap model [28]. The inset of Fig. 3(a) represents the corresponding activation energy spectra $P(E)$ (see Ref. [24]

for details) of Zr₅₀Cu₄₀Al₁₀ preaged at $0.8T_g$ for 3 h and longer time. Upon preaging, the spectra shift towards the high-energy side, indicative of the increasing activation energy of individual flow units. For the preaged Zr₅₀Cu₄₀Al₁₀, the flow behaviors at $0.825T_g$ and $0.85T_g$ were also investigated and are shown in Fig. 3(b). As T increases, the characteristic time shows a substantial decrease, but the stretched exponential behavior with the particular value of $\beta = 3/7$ is still well followed. Thus it is obvious that the properly aged MGs follow a stretched exponential flow behavior with, in particular, a $3/7$ stretching exponent, without loss of generality. The activation energy spectra in the inset of Fig. 3(b) show no notable change with temperature, consistent with the Arrhenius behavior of temperature-independent activation energy (2.67 eV; see Fig. S7 [24]).

In Fig. 2(b), the VFT fit to the equilibrium relaxation time τ_α of Zr₅₀Cu₄₀Al₁₀ MG implies that the relaxation time will become infinite around 482 K [26]. Remarkably, we observe that the glass indeed flows even at RT, although exceedingly slowly. By studying an extremely stable (20-million-year-old) fossil amber, the upper-bound relaxation time of its equilibrium dynamics at temperatures of 43.6 K below T_g had been determined to be much shorter than the VFT dependence, showing an Arrhenius behavior instead [29]. The Arrhenius (instead of VFT) behavior of equilibrium dynamics well below T_g has also been reported in a wide family of glasses obtained by physical vapor deposition, which have an anecdotal fictive temperature of dozens of degrees below T_g [30]. By directly probing the slow flow of MGs, we have shown that in such a wide temperature range Arrhenius behavior was followed in as-cast MGs [Fig. 2(b)] and also in aged MGs with larger activation energy (Fig. S7 [24]). It is thus reasonable to infer that the Arrhenius behavior persists regardless of the glassy state and, also in the equilibrium state. In that sense, our results might corroborate earlier evidence of VFT breakdown [2,29–32], ruling out the finite temperature divergence of the relaxation time directly from the extremely slow flow perspective.

Differential scanning calorimetry (DSC) is an effective way to characterize the glassy energy state change with aging. Figure 4 shows the enthalpy change ΔH of aged Zr₅₀Cu₄₀Al₁₀ MGs relative to that of as-cast sample determined directly by DSC (inset of Fig. 4). As expected, ΔH undergoes a dramatic increase (that is, a decrease of energy state) within the initial 3 h of aging. Coincidentally, after preaging for 3 h or longer, the flow behavior can be well captured by the stretched exponential function, yet the flow behaviors of as-cast and short time (45 min) aged MG are indescribable [Fig. 3(a)]. This coincidence implies a close correlation between the intrinsic mechanism of slow flow and the glassy state, as will be discussed in detail below.

The DSC trace of an as-cast MG ribbon exhibiting a broad sub- T_g exothermic peak (inset of Fig. 4) [33] and other robust evidence from both direct explorations [34–36] and atomistic simulations [37] indicate the existence of structural heterogeneity in MGs. It has been proposed that the heterogeneity in MGs represents the mixture of densely packed (solidlike) and loosely packed (liquidlike) regions [38]. Such liquidlike regions are energetically unfavorable and more prone to be activated as flow units [8,38]. In as-cast MGs, such abundant

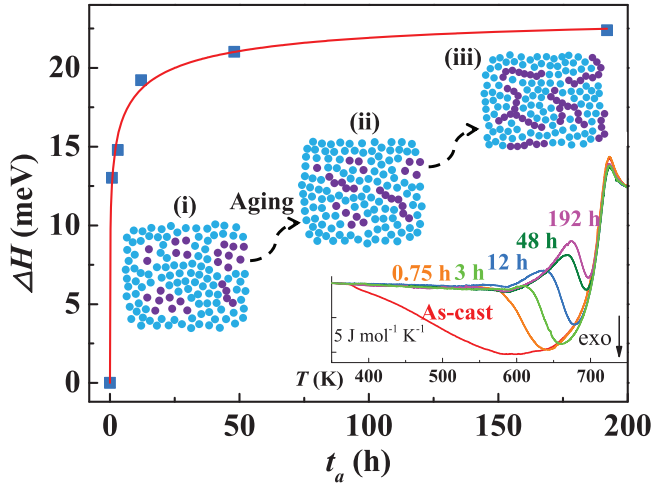


FIG. 4. Relative enthalpy change ΔH plotted against the annealing time for $Zr_{50}Cu_{40}Al_{10}$ MGs at $0.8T_g$. The red line represents a good fit using a stretched exponential function with a relaxation time of 2 h and a stretching exponent of 0.263. The insets show the DSC curves at a heating rate of 20 K/min, and a schematic of the evolution of the atomic configurations of flow units (violet circles) during aging.

flow units can be effortlessly activated and contribute to the macroscopic homogeneous flow, even leading to avalanchelike flow behavior at higher temperatures [Fig. 2(a)]. Additionally, the activation energy is in good accordance with that of SL, implying a similar origin for flow in glass and SL. The results quantitatively imply that the glass transition can be considered as a freezing into an energy minimum of a certain SL state [39], although the distribution of frozen-in energies may deviate from the equilibrium distribution [40].

The stretched exponential function is capable of describing many data in disordered systems, e.g., in (as-cast) MGs the exponent is generally regarded to be related to the heterogeneity [14], but no microscopic physical meaning can be assigned to it. A major breakthrough in understanding the physical origin of the stretched exponential relaxation can be found in the diffusion-trap model [28]. According to this model, the corresponding flow arises from local excitations that are distributed homogeneously and relax by diffusion to the randomly distributed traps (or sinks), which capture and absorb the excitations. The neighborhoods of the traps are progressively depleted, and at later times excitations must diffuse larger distances to reach the traps and be captured, and stretched exponential behavior is thus produced. The stretching exponent is simply related to the effective dimensionality D^* of relaxation channels by $\beta = D^*/(D^* + 2)$. With all channels in action, $D^* = 3$ and $\beta = 3/5$ is derived. While for the case of mixed short- and long-range forces, an assumption of equipartitioning of the two relaxation channels yields a fractal dimensionality of $D^* = 3/2$ for the long-range relaxation pathways. Then one obtains $\beta = 3/7$ for relaxation governed by long-range interactions [28]. A stretched exponential flow with the $3/7$ exponent has previously been observed in an industrial silicate glass, where homogeneously distributed alkali ions are regarded as the source of long-range interactions of Coulomb forces [7]. Another existing example

is amorphous Se, which is fitted with the $3/7$ exponent and has long spiral chains [28]. The flow behaviors of aged MGs which can be accurately modeled by a stretched exponential function with the particular stretching exponent of $3/7$ suggest this as well. For the case of MGs, in the absence of additional Coulomb forces or other long-range strong interactions, a cooperative stringlike configuration seems plausible as the source of localized atomic mobility. Such atomic strings can move back and forth reversibly and cooperatively. Once activated, strong coupling between one end of the atomic string and the other is spontaneously established, and it is reasonable to consider it as the source of long-range interactions governing the relaxation pathways; consequently, the particular $3/7$ stretching exponent is obtained.

Our results might provide insight into the in-depth mechanisms of the contrasting flow behaviors of highly heterogeneous (as-cast) and relatively homogeneous (properly aged) MGs. In the former case, the MG contains a large amount of the flow units [illustrated in case (i) in the inset of Fig. 4], within which the atoms are relatively mobile and likely to rearrange with weak interaction, albeit collectively. Such flow units frozen in from SL are effortlessly activated and lead to the observed fast homogeneous flow in as-cast MGs as shown in Fig. 2(a). With aging, the MG gradually relaxes towards a more homogeneous state [33], e.g., aging of a Zr-based MG at $0.85T_g$ for just 30 min has been found to induce dramatic homogenization [34]. In the absence of large as-cast heterogeneity, correlation between atoms becomes significant [34,41], and the cooperative stringlike configuration gradually takes over and emerges as the dominant relaxation event with long-range end interactions [case (iii) in the inset of Fig. 4], leading consequently to a stretched exponential relaxation with the particular value of $\beta = 3/7$. Consistent with this scenario, convincing evidence has been provided [42–45] demonstrating that relaxations in glass are related to cooperative stringlike atomic motions.

In summary, slow dynamics in MGs was scrutinized from the homogeneous flow perspective ranging from T_g to RT and spanning more than 1 month. For as-cast MGs, the flow dynamics follows a universal Arrhenius behavior, from T_g to the temperature well below the dynamic divergence predicted by the VFT equation. The activation energy for flow in as-cast glass is similar to that of SL, indicating a freezing of potential energy barriers during the liquid to glass transition. We find that the stretched exponential relaxation with $\beta = 3/7$ is intrinsic for aged MGs, which allows for plausible speculation of the relaxation mechanism being dominated by a cooperative stringlike configuration. These observations advance the understanding of the physical origin of stretched exponential relaxation, and imply an evolutionary picture of atomic rearrangement of flow units from a collective motion of a nearly randomly packed atomic group to a cooperative stringlike configuration with aging.

We thank J. C. Phillips and J. C. Mauro for correspondence, and M. Gao, R. J. Xue, and D. Q. Zhao for experimental assistance. This work was supported by the NSF of China (Grant No. 51271195) and MOST 973 Program (Grant No. 2015CB856800).

- [1] E. D. Zanotto, *Am. J. Phys.* **66**, 392 (1998); E. D. Zanotto and P. K. Gupta, *ibid.* **67**, 260 (1999); R. H. Brill, *Glass Worldwide* **8**, 12 (2006).
- [2] T. Hecksher, A. I. Nielsen, N. B. Olsen, and J. C. Dyre, *Nat. Phys.* **4**, 737 (2008).
- [3] K. L. Ngai, *Relaxation and Diffusion in Complex Systems* (Springer, New York, 2011).
- [4] G. B. McKenna, *Nat. Phys.* **4**, 673 (2008).
- [5] G. P. Johari and M. Goldstein, *J. Chem. Phys.* **53**, 2372 (1970).
- [6] C. A. Angell, K. L. Ngai, G. B. McKenna, P. F. McMillan, and S. W. Martin, *J. Appl. Phys.* **88**, 3113 (2000).
- [7] R. C. Welch, J. R. Smith, M. Potuzak, X. J. Guo, B. F. Bowden, T. J. Kiczanski, D. C. Allan, E. A. King, A. J. Ellison, and J. C. Mauro, *Phys. Rev. Lett.* **110**, 265901 (2013); M. Micoulaut, *Physics* **6**, 72 (2013).
- [8] W. H. Wang, *J. Appl. Phys.* **99**, 093506 (2006).
- [9] Z. Lu, W. Jiao, W. H. Wang, and H. Y. Bai, *Phys. Rev. Lett.* **113**, 045501 (2014).
- [10] J. S. Harmon, M. D. Demetriou, W. L. Johnson and K. Samwer, *Phys. Rev. Lett.* **99**, 135502 (2007).
- [11] H. B. Yu, W. H. Wang, H. Y. Bai, Y. Wu, and M. W. Chen, *Phys. Rev. B* **81**, 220201(R) (2010).
- [12] H. B. Yu, X. Shen, Z. Wang, L. Gu, W. H. Wang, and H. Y. Bai, *Phys. Rev. Lett.* **108**, 015504 (2012).
- [13] P. Luo, Z. Lu, Z. G. Zhu, Y. Z. Li, H. Y. Bai, and W. H. Wang, *Appl. Phys. Lett.* **106**, 031907 (2015).
- [14] Z. Wang, B. A. Sun, H. Y. Bai, and W. H. Wang, *Nat. Commun.* **5**, 5823 (2014); Y. Z. Li, L. Z. Zhao, C. Wang, Z. Lu, H. Y. Bai, and W. H. Wang, *J. Chem. Phys.* **143**, 041104 (2015).
- [15] H. B. Yu, K. Samwer, and W. H. Wang, *Phys. Rev. Lett.* **109**, 095508 (2012).
- [16] P. Wen, D. Q. Zhao, M. X. Pan, and W. H. Wang, *Appl. Phys. Lett.* **84**, 2790 (2004).
- [17] L. N. Hu and Y. Z. Yue, *J. Phys. Chem. C* **113**, 15001 (2009).
- [18] Z. F. Zhao, P. Wen, and W. H. Wang, *Phys. Rev. B* **75**, 174201 (2007).
- [19] H. B. Yu, W. H. Wang, and K. Samwer, *Nat. Sci. Rev.* **1**, 429 (2014).
- [20] Z. G. Zhu, Y. Z. Li, Z. Wang, X. Q. Gao, P. Wen, H. Y. Bai, K. L. Ngai, and W. H. Wang, *J. Chem. Phys.* **141**, 084506 (2014).
- [21] J. C. Qiao, R. Casalini, and J. M. Pelletier, *J. Phys. Chem. B* **118**, 3720 (2014).
- [22] B. A. Sun, S. Pauly, J. Hu, W. H. Wang, U. Kühn, and J. Eckert, *Phys. Rev. Lett.* **110**, 225501 (2013).
- [23] J. J. Lewandowski and A. L. Greer, *Nat. Mater.* **5**, 15 (2006).
- [24] See Supplemental Material at <http://link.aps.org/supplemental/10.1103/PhysRevB.93.104204> for experimental details and additional information.
- [25] P. A. O'Connell and G. B. McKenna, *Polym. Eng. Sci.* **37**, 1485 (1997).
- [26] H. Vogel, *Phys. Zeit.* **22**, 645 (1921); G. S. Fulcher, *J. Am. Ceram. Soc.* **8**, 339 (1925); G. Tammann and W. Hesse, *Z. Anorg. Allg. Chem.* **156**, 245 (1926).
- [27] I. M. Hodge, *Science* **267**, 1945 (1995).
- [28] J. C. Phillips, *Rep. Prog. Phys.* **59**, 1133 (1996); G. G. Naumis and J. C. Phillips, *J. Non-Cryst. Solids* **358**, 893 (2012).
- [29] J. Zhao, S. L. Simon, and G. B. McKenna, *Nat. Commun.* **4**, 1783 (2013).
- [30] E. A. A. Pogna *et al.*, *Proc. Natl Acad. Sci. USA* **112**, 2331 (2015).
- [31] Z. Wojnarowska, K. L. Ngai, and M. Paluch, *J. Chem. Phys.* **140**, 174502 (2014).
- [32] Y. S. Elmatad *et al.*, *J. Phys. Chem. B* **113**, 5563 (2009).
- [33] J. C. Mauro, S. S. Uzun, and S. Sen, *Phys. Rev. Lett.* **102**, 155506 (2009).
- [34] Y. H. Liu, D. Wang, K. Nakajima, W. Zhang, A. Hirata, T. Nishi, A. Inoue, and M. W. Chen, *Phys. Rev. Lett.* **106**, 125504 (2011).
- [35] H. Wagner, D. Bedorf, S. Küchemann, M. Schwabe, B. Zhang, W. Arnold, and K. Samwer, *Nat. Mater.* **10**, 439 (2011).
- [36] Z. Wang, P. Wen, L. S. Huo, H. Y. Bai, W. H. Wang, *Appl. Phys. Lett.* **101**, 121906 (2012).
- [37] J. Ding, S. Patinet, M. L. Falk, Y. Cheng, and E. Ma, *Proc. Natl Acad. Sci. USA* **111**, 14052 (2014).
- [38] S. T. Liu, W. Jiao, B. A. Sun, and W. H. Wang, *J. Non-Cryst. Solids* **376**, 76 (2013).
- [39] M. Goldstein, *J. Chem. Phys.* **51**, 3728 (1969); F. H. Stillinger and T. A. Weber, *Phys. Rev. A* **28**, 2408 (1983).
- [40] J. C. Dyre, *Rev. Mod. Phys.* **78**, 953 (2006).
- [41] C. Brun *et al.*, *Phys. Rev. Lett.* **109**, 175702 (2012).
- [42] H. R. Schober, *Physica A (Amsterdam)* **201**, 14 (1993).
- [43] J. D. Stevenson and P. G. Wolynes, *Nat. Phys.* **6**, 62 (2010).
- [44] Y. Cohen, I. Procaccia, and K. Samwer, *Europhys. Lett.* **100**, 36003 (2012).
- [45] K. H. Nagamanasa *et al.*, *Nat. Phys.* **11**, 403 (2015).